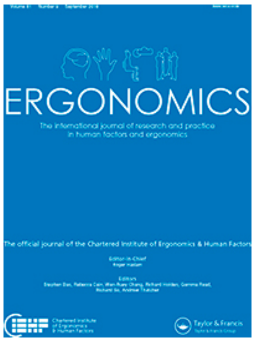

Ergonomics

ISSN: 0014-0139 (Print) 1366-5847 (Online) Journal homepage: https://www.tandfonline.com/loi/terg20

Parametric human modelling to determine body surface area covered by sun-protective clothing

Leyde Briceno, Simone Lee Harrison, Clare Heal, Michael Kimlin & Gunther Paul

To cite this article: Leyde Briceno, Simone Lee Harrison, Clare Heal, Michael Kimlin & Gunther Paul (2019): Parametric human modelling to determine body surface area covered by sun-protective clothing, Ergonomics, DOI: 10.1080/00140139.2019.1699952

To link to this article: https://doi.org/10.1080/00140139.2019.1699952

Parametric human modelling to determine body surface area covered by sun-protective clothing

Leyde Briceno[a,b], Simone Lee Harrison[b], Clare Heal[b], Michael Kimlin[c] and Gunther Paul[a,b*]

[a] *Australian Institute of Tropical Health and Medicine (AITHM), Mackay QLD 4740, Australia;* [b] *James Cook University, Townsville QLD 4811;* [c] *University of the Sunshine Coast, Sippy Downs QLD 4556*

*Corresponding author: gunther.paul@jcu.edu.au

Parametric human modelling to determine body surface area covered by sun-protective clothing

Solar ultraviolet radiation (UVR) is the main environmental risk-factor for cancer of the skin. Sun-protective clothing provides a physical barrier that reduces the UVR dose reaching the skin and European and Australian standards for sun-protective clothing set minimum clothing coverage requirements. Body Surface Area Coverage by clothing (BSAC) is calculated by means of indirect or direct methods, which are laborious and do not support computer-based apparel design. To support the sun-safe specification and design of garments, parametric digital human models and protective clothing mesh covering the minimum Body Surface Area specified in AS/NZS 4399:2017, were created making use of MakeHuman v1.1.1 and Blender software. The Whole Body Surface Area (WBSA) and the BSAC were calculated employing code developed in Blender. Thus, different groups of subjects were analysed to explore BSAC. The method assists in the evaluation of exposed body areas in a wider spectrum of different occupations.

Keywords: digital human modelling; body surface area coverage by clothing; whole body surface area; skin cancer; MakeHuman

Subject classification codes:

Practitioner summary

Sun-protective clothing provides a physical barrier that reduces the UVR dose reaching the skin’s surface. Body Surface Area Coverage (BSAC) by clothing is an important determinant of the sun protective capabilities of a garment. In this study, BSAC is calculated using parametric digital human modelling.

Introduction

Solar ultraviolet radiation is a known carcinogen (IARC 1992). It is the main environmental risk-factor for cancer of the skin, of which there are three major types: basal cell carcinoma (BCC); squamous cell carcinoma (SCC); and, malignant melanoma, which develops in the pigment producing cells (melanocytes) and is more likely to metastasize than the other types of skin cancer (IARC 1992; Lucas et al 2006).

Skin cancer is the most common form of cancer in Caucasian populations world-wide (IARC 1992; Lucas et al 2006), as well as being the most expensive in terms of direct costs to the health system (Doran et al 2015). However, theoretically, it is the easiest form of cancer to prevent and easier than internal cancers to detect and treat early, because the warning signs manifest on the surface of the skin where they can easily be observed (Lucas et al 2006; Armstrong and Kricker 1993).

The risk of all three types of skin cancer increases with higher ambient solar radiation, such that the highest densities are found on the most sun exposed parts of the body and the lowest on the least exposed. This applies equally to associations in individuals with total or occupational (SCC dominant), and non-occupational or recreational sun exposure (melanoma and BCC dominant) (Armstrong and Kricker 2001). While the highest density of non-melanocytic skin cancer is found on the face, BCC are most prevalent on the face and trunk, including shoulders; and SCC are more frequent on upper and lower extremities (Heal et al 2008).

A randomized trial demonstrated a small, significant reduction of new pigmented moles (the strongest predictors of melanoma risk) in Canadian schoolchildren with summer sunscreen use (Gallagher et al 2000) and recent follow-up of a community-based trial conducted in Queensland-Australia suggests that long-term daily sunscreen use can prevent primary cutaneous melanoma in Caucasian adults

(Green et al 2011). Despite its apparent efficacy in preventing SCC (van der Pols et al 2006), pigmented moles (Gallagher et al 2000) and melanoma (Green et al 2011), sunscreen is more prone to incorrect use than clothing (Harrison, Buettner, and MacLennan 2005). Applying too little sunscreen or not re-applying the product often enough is known to significantly reduce its effectiveness (Stokes and Diffey 1997; Diffey 2001). On the other hand, sun-protective clothing such as brimmed hats, sleeved shirts, nylon elastane rash-vests, and all-in-one protective swimsuits provide a physical barrier that reduces the amount of UVR reaching the skin (Harrison and Downs 2015), without the challenges associated with the incorrect application of chemical sunscreens (Stokes and Diffey 1997; Diffey 2001; Harrison, Buettner, and MacLennan 2005).

In 1996, Australia pioneered a reproducible measurement and classification protocol based on the relative ranking of UVR transmittance through fabric, known as the ultraviolet Protection Factor (UPF) (Gies et al 1994). This led to the publication of AS/NZS 4399:1996, the joint Australian and New Zealand Standard for the evaluation and classification of sun-protective clothing (AS/NZS 1996). The original Standard also provided specifications for UPF labels for garments and fabrics wishing to claim a sun-protective advantage (AS/NZS 1996). Industry standards modelled on AS/NZS 4399:1996 have since been implemented in Britain, Europe, and the USA (BS 1999; CSN EN 2003; AATCC 2014; ASTM 2012).

AS/NZ 4399:1996 and its associated UPF rating system were adopted almost universally by the textile industry (AS/NZS 1996). However, the original standard only considered the UVR transmittance of the fabric, without taking into consideration the proportion of the BSA covered by the garment (Harrison and Downs 2015). In recent years, it became apparent that manufacturers were potentially misleading consumers by displaying UPF labels on brief swimwear and apparel because most of these garments or swimwear were made of fabrics with high UPF ratings even though they cover very little skin (Harrison and Downs 2015).

Minimum clothing coverage standards are specified in the European Standard for sun-protective clothing (CSN EN 2003) and the 2017 revision of the joint Australian/New Zealand Standard for the evaluation and classification of sun-protective clothing (AS/NZS 4399:2017) (AS/NZS 2017). In Australia and New Zealand, only those garments meeting or exceeding the minimum clothing coverage standards specified in AS/NZS 4399:2017 are able to display a UPF label or claim a sun-protective advantage (AS/NZS 2017).

A new index for sun-protective clothing called "the Garment Protection Factor (GPF)" which simultaneously considers BSAC and fabric UPF was recently proposed (Downs and Harrison 2018). A GPF greater than or equal to zero can only be achieved by meeting the minimum requirements of these standards (Downs and Harrison 2018). In addition to ensuring that both the BSAC of a garment and the UPF of the fabric are taken into consideration when evaluating sun-protective clothing, adoption of the GPF or a similar comprehensive index in future sun-protective clothing standards may provide an incentive for clothing manufacturers to design garments with higher BSAC, as these yield higher GPF values indicative of a better sun-protective rating (Downs and Harrison 2018).

Until such a comprehensive index is adopted, fabric UPF and the BSAC should be reported separately on the swing tag so that it is easier for consumers to compare both of the components that determine the sun-protective capability for different garments.

Gage et al (2017) have calculated the body coverage of 38 clothing items using diagrams of BSA, observations and self-report information. They have pointed out that due the large variety of clothing items and styles clothing coverage might be assessed using simulation models, which would support Vogel et al (2017), who observed the potential for better sun protection behaviour, such as improved clothing to reduce recurring melanoma risk in melanoma survivors. Raasch et al (1998) however pointed out that typical data on body site distribution of BCC and SCC did not account for the surface proportion occupied by body sites subjected to heterogeneous levels of UVR, and that recordings of BCC, SCC and body sites were not standardized.

As a result of the lack in standardised methods for determining BSA and body sites, and to support the sun-safe specification and design of garments, this study explores a procedure to calculate BSAC and Whole Body Surface Area (WBSA) using a digital human modelling approach, standard anthropometric dimensions, definitions from the Australian Standard and free open-source digital human modelling (DHM) programs. A validation is carried out to test the relationship between our variables proposed to predict BSAC or WBSA and published data, exploring the feasibility to use free open-source software programs such as MakeHuman and Blender to compute BSAC.

Materials and methods

Virtual Human dataset

A dataset was created which constituted of 288 virtual subjects; which were stratified by gender (male and female), age groups (20-80 yrs), height (5th, 50th, and 95th percentiles) and waist circumference (5th, 50th, and 95th percentiles).

This study was guided by stature (height) and waist circumference as predictors of WBSA and was presented in Briceno, Harrison and Paul (2018). This model is now called Model 1, and is updated and extended to form Model 2. The models present two approaches for transforming absolute anthropometric values (i. e. body measurements) into normed relative values [0, 1] used in the MakeHuman software system. In model 1 we identified functions among parameters by 5th, 50th and 95th waist circumference percentiles, while additional parameters (e.g. ethnicity) and relationships (Figure 3) were considered in model 2 to further improve model accuracy and reliability, and functions were thus converted into algorithms. In this way the MakeHuman template model was expanded to DHM datasets. Our approach is to incorporate the indices calculated using Model 1 and Model 2 into the MakeHuman software program, deforming the template meshes on the MakeHuman models to specific body size.

MakeHuman v1.1.1 software (Bastioni and Misra 2008) and the US National Health and Nutrition Examination Survey (NHANES) (Fryar et al 2016) were used to generate virtual human datasets. The MakeHuman parametric model is based on fuzzy logic, which through membership functions or rules assign a value [0, 1] to each element that belongs to a fuzzy set; each fuzzy set contains all the possible values under consideration (Zadeh 1999). Consequently, anthropometric data must be transformed to relative values [0, 1].

Procedures were developed and implemented in a Blender script in order to get the indices. Height index was calculated reading from tables the minimum, average and maximum height values (Figure 1), which change by gender, age and ethnicity factor. By means of the membership function (Equation 1) height values were determined and related to the index [0, 1] (Figure 2). The index for a specific stature was obtained by interpolation. Weight and muscle indices have been obtained analysing the patterns found by gender, age, height percentile (5th, 50th, and 95th) and waist circumference percentile (5th, 50th, and 95th).

$$(minI*minPV) + (aveI*avePV) + (maxI*maxPV) = PV \tag{1}$$

minI: minimum index

minPV: minimum parameter value

aveI: average index

avePV: average parameter value

maxI: maximum index

maxPV: maximum parameter value

PV: parameter value

[Figure 1 near here]

[Figure 2 near here]

Waist circumference index was obtained reading tables from minimum, average and maximum waist circumference values which depend on gender, age and minimum, average and maximum height values (Figure 3). The index value was determined as an interpolation for a given waist circumference value.

[Figure 3 near here]

Two variations of ethnicity index were used: Caucasian (African = 0, Asian = 0, Caucasian = 1) and Ethic group equally represented (African = 0.3333, Asian = 0.3333, Caucasian = 0.3333).

Sun protective clothing

The sun protective clothing type ‘all-in-one’ was reproduced using MakeHuman add-ons in Blender and definitions from the Australian Standard AS/NZS 4399:2017, following the procedure to generate the ‘all-in-one’ clothing proposed by Briceno, Harrison and Paul (2018). ‘All-in-one’ clothing covers the body from the neck point to halfway between crotch and knee and has sleeves that cover three-quarters of the length between the shoulder point and elbow. One template mesh was created for each gender, then during the assembling process, it was deformed to fit the body shape of each subject (considering correct sizing of clothing, the material is not stretched) and the set of body vertices covered by clothing were deleted.

Body surface area

WBSA was defined as the sum of the surfaces of all n elements (Equation 2) on the whole outer body surface; the set of vertices associated with body cavities were removed during the body generation process. Body Surface Area Not Covered by clothing (BSANC) is the sum of the surfaces of all m elements (Equation 3) on the body surface not covered by clothing surface. BSAC was calculated as the difference between WBSA and BSANC. The body mesh featured quadrilateral elements with 12,346 vertices and 12,300 faces for the full uncovered body. The procedure was implemented in a Blender script.

$$WBSA = \sum_{i=1}^{n} e_i \qquad (2)$$

$$BSANC = \sum_{i=1}^{m} e_i \qquad (3)$$

Data analysis

Separate analyses using the same procedure were accomplished for each gender and waist circumference percentile (5th, 50th, and 95th). Plots and analyses were performed using R software. Spearman’s correlation and Pearson correlation coefficients were used to analyse relationships between parameters and surface areas. Boxplots, Levene’s test for homogeneity of variance (null hypothesis: groups variances are equal, α=0.05) and the Mann-Whitney U test for independent groups (null hypothesis: distributions differ by μ=0, two-sided, α=0.05) were used in the comparison of model 1 and 2 output with results from Lee, Choi and Kim (2008). The effect size for the Mann-Whitney U test is estimated using the Glass rank-biserial correlation (Equation 4) (Tomczak and Tomczak, 2014) and the formula stated by Kerby (2014) for the correlation as the difference between the proportion of favourable and unfavourable evidence (Equation 5).

$$r = \frac{2*(\overline{R_1} - \overline{R_2})}{n_1 + n_2} \quad (4)$$

$\overline{R_1}$: mean rank for group 1

$\overline{R_2}$: mean rank for group 2

n_1: sample size (group 1)

n_2 : sample size (group 2)

r: correlation coefficient {-1 ≤ r ≤ 1}

$$r_k = \frac{P}{P_{max}} - \frac{Q}{P_{max}} \quad (5)$$

P: number of favourable pairs

Q: number of unfavourable pairs

P_{max}: maximum value

Mesh error and validation

For mesh error analysis, we chose distance computation and it was evaluated against data from Mitsuhashi et al (2008). The validation was carried out using data from Lee, Choi and Kim (2008).

Distance computation

Distance computations were performed using the two-sided Hausdorff distance (d_H) (Cignoni, Rocchini and Scopigno 1998) and a distance surface map from Multiscale

Model to Model Cloud Comparison (M3C2) (Lague, Brodu and Leroux 2013), where d_H is widely used to compare two mesh surfaces, providing a global comparison. This method can compare meshes even if the levels of detail are different (Lavoué and Corsini 2010). M3C2 is computed in order to evaluate 3D variations in surface orientation as well as estimate local distance measurement accuracy. This method is able to measure surface changes independent of point density and surface roughness (Lague, Brodu and Leroux 2013).

Hausdorff distance (d_H) computation was performed using MeshLab (v2016.12 on Intel Core i5-7600, 3.50 GHz, 8 GB RAM, 237 GB) (Cignoni, Rocchini and Scopigno 1998) and M3C2 using CloudCompare (v2.10.2 Zephyrus on Intel Core i5-7600, 3.50 GHz, 8 GB RAM, 237 GB) (Girardeau-Montaut 2011) from the scanned human body (Mitsuhashi et al 2008) to a correspondent DHM subject in MakeHuman, which was reproduced using measurements obtained from the scanned body.

The scanned body represents the skin of a Japanese adult male, as a high-quality mesh obtained from the Bodyparts3D dictionary-type database (© The Database Center for Life Science, licensed under CC Attribution-Share Alike 2.1 Japan) (Mitsuhashi et al 2008). The body mesh is constituted of triangular elements with 53,851 vertices. The inner shell and genitals were removed and only the outer shell (epidermis) was conserved in order to be compatible with the MakeHuman body mesh.

The body mesh stature was measured as the maximum length of the mesh bounding box size utilising Compute Geometric Measures in MeshLab software (Cignoni et al 2008). Upper arm length, upper leg length, minor and major diameter (waist circumference and upper arm circumference) were measured using the point to point tool. Circumference measurements were calculated as the perimeter of an ellipse and confirmed using the GiD graphical preprocessor (CIMNE, Campus Nord UPC).

In a pre-processing step, the pose was applied through the MakeHuman Blender tools. We scaled both models into similar height, changing the DHM subject from [dm] to [mm] in Blender. The two meshes were aligned to be matched using matrix transformations (rotations, translations) in MeshLab.

Validation data

To demonstrate the validity of our method, our results were compared with related existing reference data from Lee, Choi and Kim (2008). In their work, BSA was determined using the traditional alginate method. Their dataset is constituted of Korean people, 31 women (age: 20-63 yrs) and 34 men (age: 20-60 yrs). In our study, this dataset was filtered in order to separate subjects who matched with 5th, 50th and 95th percentiles of stature and weight, stratified by gender and age group,

The subjects were selected combining information from US population percentiles (height and weight) and connected dimensions (height and weight) by means of PeopleSize software (Open Ergonomics, Melton Mowbray); as well as, the body shape groups reported by Lee, Choi and Kim (2008).

Results

The following sections present the results using the procedures proposed in model 1 and 2, as well as the measures of model performance.

Model 1

Figures 4 and 5 display Spearman's correlations between parameters and WBSA for the 50th percentile waist circumference index (P50), which shows that WBSA is correlated with height index (corr(h,WBSA) $_{Female}$ = 0.912, p** < 0.001; corr(h,WBSA) $_{Male}$ = 0.952, p** < 0.001) and waist circumference index (corr(wc,WBSA) $_{Female}$ = -0.603,

$p^{**} = 0.004$; corr(wc,WBSA) $_{Male} = -0.631$, $p^{**} = 0.002$).

[Figure 4 near here]

[Figure 5 near here]

Model 2

Figures 6 and 7 show that WBSA is correlated with height index (corr(h,WBSA) $_{Female} =$ 0.91, $p^{**} < 0.001$; corr(h,WBSA) $_{Male} = 0.949$, $p^{**} < 0.001$) and to a lesser extent with waist circumference index (corr(wc,WBSA) $_{Female} = -0.6376$, $p^{**} = 0.002$; corr(wc,WBSA) $_{Male} = -0.5557$, $p^{**} = 0.009$).

[Figure 6 near here]

[Figure 7 near here]

Pearson's correlation was used to measure the relation between WBSA and BSAC. For females (Figure 8(a), 8(b) and 8(c)) and males (Figure 8(d), 8(e) and 8(f)) wearing 'all-in-one' clothing, linear relationships were found between WBSA and BSAC by gender and waist circumference percentile. Furthermore, BSA covered by 'all-in-one' clothing are presented in Table 1.

[Figure 8 a), b), c), d), e), f) near here]

[Table 1 near here]

Mesh error and validation

Distance computation

The Hausdorff distance (d_H) was calculated by sampling 53,851 vertices on the scanned body and measuring distances from the nearest faces on the DHM subject (model 2, ethnic groups represented equally). The mean Hausdorff distance was $d_H = 8.42$ mm (0.0002 mm $< d_H <$ 38.93 mm; $d_{HRMS} = 11.11$ mm) and the bounding box diagonal mean difference was d = 0.005 mm (d_{RMS} = 0.006 mm).

The Multiscale Model to Model Cloud Comparison distance (d_{M3C2}) was calculated between both point clouds ($\overline{d}_{M3C2} = 0.574$ mm, σ_{M3C2}= 18.646 mm). Figure 9 shows the distance map between the scanned body and the DHM subject, where distances are represented at each point on the compared cloud.

[Figure 9 near here]

Validation against Lee, Choi and Kim (2008)

Four datasets for both genders were created using the proposed models and variations of ethnicity factor (datasets nomenclature, see Table 2).

Since the value of the Levene's test for homogeneity of variance (centre = median) at a confidence level of 5% was less than the critical value for both female ($F_{upper}(0.05, 1, 9) = 5.12$; Fm1c: F = 2.22; Fm1m: F = 2.44; Fm2c: F = 2.16; Fm2m: F = 2.66) and male ($F_{upper}(0.05, 1, 10) = 4.97$; Mm1c: F = 0.12; Mm1m: F = 0.21; Mm2c: F = 0.13; Mm2m: F = 0.14), the assumption of homogeneity of variance between the comparison groups is satisfied.

Results of the two-sided Mann-Whitney U test at 5% confidence level showed no evidence that the groups differ for females (m = 5, n = 6; $3 \leq U \leq 27$; U_{Fm1c} = 15, r = 0, interval 95% (-25.7, 33.51); $U_{Fm1m} = U_{Fm2c} = U_{Fm2m}$ = 14, r = 0.067) and males (m = 5, n = 7, $5 \leq U \leq 30$; $U_{Mm1c} = U_{Mm2c}$ = 15, r = 0.14; U_{Mm1m} = 16, r = -0.086; U_{Mm2m} = 17, r = 0.029).

Using Kerby's (2014) formula for comparing WBSA among DHM subjects and the results reported by Lee, Choi and Kim (2008) (Table 2). For Fm1c, it is shown that the scales are not tipped either way, whilst in other female DHM subject variations the

WBSA were smaller. For male DHM subject variations, Mm2m shows the lowest difference, while Mm1c and Mm2c present the largest differences.

[Table 2 near here]

Distributions of WBSA by DHM subjects and the results reported by Lee, Choi and Kim (2008) are shown in Figures 10 (a, b, c, d) and 11 (a, b, c, d).

[Figure 10 a), b), c) y d) near here]

[Figure 11 a), b), c) y d) near here]

Discussion

We found that BSAC is highly correlated with the WBSA for both genders and all waist circumference percentiles (Figure 8). Moreover, our results show differences in BSAC covered by 'all-in-one' among genders and waist circumference percentiles (5^{th}, 50^{th}, and 95^{th}) with increasing age, as well as a higher percentage of coverage for women (Table 1). Those outcomes could be associated with different levels of body fat by sex and age. Some studies have found correlations of adiposity for sex and age group (Bosy-Westphal et al 2006; Flegal et al 2009); while waist circumference is slightly more correlated with fat among men but slightly less among women (Flegal et al 2009). Despite this, several studies suggest that BSAC differences associated with body shape and between genders are not significant (Yu, Lo and Chiou 2003; Lee, Choi and Kim 2008).

Our results for WBSA were obtained using as input two anthropometric variables (stature and waist circumference), gender (female, male), age (20-80 yrs) and the functions found for age, weight and muscle indices by 5^{th}, 50^{th} and 95^{th} waist circumference percentile. Most researchers however have only reported height and weight as predictors of WBSA (Du Bois and Du Bois 1916; Sendroy and Collison 1954; Gehan and George 1970; Yu, Lo and Chiou 2003; Lee, Choi and Kim 2008).

Model 1 showed a higher correlation between WBSA, height index (both genders) and waist circumference index (male gender) compared to model 2 (Figures 4, 5, 6 and 7). Subjects below 20 years of age were excluded from those analyses, because they exhibited different parameter patterns.

DHM datasets were derived by defining waist circumference classes as percentile range, and varying height percentiles by age group. Thus, when height was increased, WBSA increased proportionally, but waist circumference remained at the specified value. Due to the interdependency among parameters in the MakeHuman modelling framework, this can be achieved by reducing the waist circumference index value. Consequently, negative correlations between WBSA and waist circumference index were found.

To test our approach, we used two comparison metrics. Firstly, an average global distance (d_H = 8.42 mm), where the bounding box diagonals differ in length by less than 1%. When two bounding box diagonals differ by more than 10%, it is considered an excessive error (Cignoni, Rocchini and Scopigno 1998). However, discrepancies of any part of the surface cannot be quantified with only a single value and this result can be affected by numerical calculations, differences between mesh alignments, occlusions and noisy input data (Iannessi et al. 2018; Drakopoulos 2007). Secondly, a point cloud comparison ($\overline{d}_{M3C2}$ =0.574 mm) and distance map was calculated for the whole-body point cloud, showing the similarity between the scanned body and the DHM subject and allowing identification of local discrepancies. As shown in Figure 9, the DHM subject captures shape variation, even though, it exhibits underestimation around chest circumference and overestimation in the back of the upper arms and fingers. Overestimations might be associated with an error between coordinate systems of the two clouds, although those values are found in areas of high degrees of curvature, where the measurement method might report erroneous distances. In contrast, underestimations of the chest region might suggest that this dimension is required in the set of parameters to fully describe the body shape. Further analyses are needed.

The validation carried out between this study (Table 2) and results from Lee, Choi and Kim (2008) for subjects matched by gender, age group, height and weight / waist circumference percentile (based on the US population NHANES) did not indicate significant differences between group distributions. Though, sample sizes were smaller than 10 subjects, which might inflate type II errors. The smallest median of the WBSA differences was 0.095 dm^2 for females (Fm1c) and 0.102 dm^2 for males (Mm2m), indicating that there is not one general model and that the model selection should be adjusted for gender and ethnic group to be applicable to other populations. Pheasant (1996) however suggested that the variations of body dimensions of different ethnic groups could be observed overall.

Due to the lack of data, this comparison was not representative of the population beyond the 95^{th} percentile height and waist circumference. In view of that, studies including subjects from the 95^{th} percentile group are required for a more representative assessment and full validation. A validation against the CAESAR dataset may be warranted.

As mentioned earlier on, regularly wearing sun-protective clothing may influence a lower lifetime risk for developing melanoma (Harrison, Buettner, and MacLennan 2005; Harrison et al 2010); however, it is not the only skin condition for which protective clothing is useful and indicated. Other examples include: slowing skin ageing, preventing acute responses (e.g. prevent sunburn; avoid freckling/darkening of freckles) and other chronic responses to solar UVR, development of excessive numbers of pigmented moles, minimize effects of pigmentary disorders (e.g. melasma), provide sun-protection for those with photosensitivity caused by medication.

Therefore, the development of methods for determining the exact total UV dose absorbed, digitally assessing common clothing items that meet the minimum requirements as specified in the standards for sun-protective clothing (such as the transmission of erythemal effective UVR through the garment fabric and minimum garment coverage), and using real-world patterns in digital testing should be a priority of apparel design.

The results propose that the method outlined in this study and the set of anthropometric variables proposed (stature and waist circumference) can predict BSAC, enabling the use of open-source software programs such as MakeHuman and Blender to compute garment specific BSAC in commercial applications.

Making use of ergonomic digital human modelling and based on epidemiological evidence, future studies should explore whether greater coverage of skin and better sun protective capabilities of apparel influence the incidence of skin abnormalities; and research the association with other risk factors and personal sun exposure behaviour.

Conclusion

We determined WBSA and BSAC using human models generated with MakeHuman v1.1.1, employing anthropometric data from the NHANES dataset and two models proposed, which transform anthropometric measurements into relative values [0, 1]. Our results show differences in BSAC (%) between genders and waist circumference percentiles. Datasets of our DHM subjects were compared with data from Lee, Choi and Kim (2008) and Mitsuhashi et al. (2008) and based on statistical assessment we found no differences between group distributions for WBSA. However, due to limitations in sample size and spread, further validation of our model-based approach against more extensive datasets is required.

Acknowledgments

This paper is an invited and significantly extended version of the paper by Briceno, Harrison & Paul, “Towards parametric modelling of skin cancer risk: Estimation of body surface area covered by protective clothing using base mesh modelling” presented at the International Ergonomics Association triannual conference in Florence, Italy, 26.-30. August 2018, and published by Springer International Publishing under the Proceedings of the 20th Congress of the International Ergonomics Association, IEA 2018.

We thank the MakeHuman project, their software and open source code were extensive used in this study.

References

American Association of Textile Chemists and Colorists: AATCC TM183-2014 Transmittance or Blocking of Erythemally Weighted Ultraviolet Radiation through Fabrics (2014). https://members.aatcc.org/store/tm183/579/ , last accessed April 2018.

American Society for Testing and Materials: ASTM D6603-12 Standard Specification for Labeling of UV-Protective Textiles (2012). https://www.astm.org/Standards/D6603.htm, last accessed April 2018.

Armstrong, B.K., Kricker, A.: How much melanoma is caused by sun exposure? Melanoma Res. 3, 395-401 (1993).

Armstrong, B.K., Kricker, A.: The epidemiology of UV induced skin cancer. J Photochem Photobiol B. 63(1-3), 8-18 (2001).

Bastioni, M., Re, S., Misra, S.: Ideas and methods for modeling 3D human figures: The principal algorithms used by makeHuman and their implementation in a new approach to parametric modeling. In: Proceedings of the 1st Bangalore Annual Compute Conference. COMPUTE'08. New York: ACM, 10:1–10:6 (2008). https://dl.acm.org/citation.cfm?doid=1341771.1341782 , last accessed April 2018.

Bosy-Westphal, A., Geisler, C., Onur, S., Korth, O., Selberg, O., Schrezenmeir, J., Muller, M.: Value of body fat mass vs anthropometric obesity indices in the assessment of metabolic risk factors. International Journal of Obesity, 30, 475–483 (2006).

Briceno, L., Paul, G: MakeHuman: A Review of the Modelling Framework. Proceedings of the 20th Congress of the International Ergonomics Association. IEA 2018. Springer: Advances in Intelligent Systems and Computing, 822, 224-232 (2018).

Briceno, L., Harrison, S., Paul, G: Towards Parametric Modelling of Skin Cancer Risk: Estimation of Body Surface Area Covered by Protective Clothing Using Base Mesh Modelling. Proceedings of the 20th Congress of the International Ergonomics Association. IEA 2018. Springer: Advances in Intelligent Systems and Computing, 822, 106-116 (2018).

Cignoni, P., Callieri, M, Corsini, M., Dellepiane, M., Ganovelli, F., Ranzuglia, G.: MeshLab: An Open-Source Mesh Processing Tool. Sixth Eurographics Italian

Chapter Conference, 129-136 (2008). http://vcg.isti.cnr.it/Publications/2008/CCCDGR08/MeshLabEGIT.final.pdf , last accessed April 2018.

Cignoni, P., Rocchini, C., Scopigno, R.: Metro: Measuring error on simplified surfaces. Computer graphics forum. 17(2), 167-174 (1998).

Diffey, BL.: When should sunscreen be reapplied? J Am Acad Dermatol. 45(6), 882 – 885 (2001).

Doran, C.M., Ling, R., Byrnes, J., Crane, M., Searles, A., Perez, D., Shakeshaft, A.: Estimating the economic costs of skin cancer in New South Wales, Australia. BMC Public Health 15, 952 (2015).

Downs, N.J., Harrison, S.L.: A comprehensive approach to evaluating and classifying sun-protective clothing. Br J Dermatol 178, 958–64 (2018).

Drakopoulos, V. On the Computation of the Hausdorff Metric between Digitised Images in Three Dimensions. Applied Mathematics Sciences 1(4), 145-164 (2007).

Du Bois, D., Du Bois, E.F.: A formula to estimate the approximate surface area if height and weight be known. Archives of Internal Medicine. 17, 863-871 (1916).

European Committee for Standardization: CSN EN 13758-2+A1 Textiles – Solar UV protective properties – Part 2: Classification and marking of apparel (2003). https://www.en-standard.eu/csn-en-13758-2-a1-textiles-solar-uv-protective-properties-part-2-classification-and-marking-of-apparel/ , last accessed April 2018.

Flegal, K., Shepherd, J., Looker, A., Graubard, B., Borrud, L., Ogden, C., Harris, T., Everhart, J., Schenker, N.: Comparisons of percentage body fat, body mass index, waist circumference, and waist-stature ratio in adults, The American Journal of Clinical Nutrition., 89(2), 500–508 (2009).

Fryar, C.D., Gu, Q., Ogden, C.L., Flegal, K.M.: Anthropometric Reference Data for Children and Adults: United States, 2011–2014. National Center for Health Statistics. Vital and Health Statistics 3(39), (2016). https://www.cdc.gov/nchs/data/series/sr_03/sr03_039.pdf, last accessed April 2018.

Gage, R., Leung, W., Stanley, J., Reeder, A., Barr, M., Chambers, T., Smith, M., Signal, L.: Clothing protection from ultraviolet radiation: a new method for assessment. Photochemistry and Photobiology 93, 1513-1518 (2017).

Gallagher, RP., Rivers, JK., Lee TK., Bajdik, CD.,McLean DI., Coldman, AJ.: Broad-spectrum sunscreen use and the development of new nevi in white children: A randomized controlled trial. Journal of the American Medical Association 283(22), 2955-2960 (2000).

Gehan, E., George, S.: Estimation of human body surface area from height and weight. Cancer Chemotherapy reports. 54(4), 225-235 (1970).

Gies, H.P., Roy, C.R., Elliott, G., Zongli, W.: Ultraviolet radiation protection factors for clothing. Health Phys 67(2), 131-139 (1994).

Girardeau-Montaut, D. CloudCompare, A 3D point cloud and mesh processing free software. Technical Report, EDF R&D, Telecom Paris Tech, http://www.danielgm.net/cc

Green, AC., Williams, GM., Logan, V., Strutton, GM.: Reduced Melanoma After Regular Sunscreen Use: Randomized Trial Follow-Up. Journal of Clinical Oncology 29(3), 257-263 (2011).

Harrison S.L., Downs, N.: Development of a Reproducible Rating System for Sun Protective Clothing that Incorporates Body Surface Coverage. World J Eng Tech. 3, 208-214 (2015).

Harrison, S. L., Buettner, P.G., MacLennan, R.: The North Queensland Sun-Safe Clothing Study: Design and Baseline Results of a Randomized Trial to Determine the Effectiveness of Sun-Protective Clothing in Preventing Melanocytic Nevi. Am J Epidemiol 161(6), 536-545 (2005).

Harrison, S.L., Buettner, P.G., MacLennan R., Woosnam, J., Hutton, L., Nowak, M.: Sun-safe clothing helps to prevent the development of pigmented moles - Results of a randomised control trial in young Australian children. Ann ACTM 11, 49-50 (2010).

Heal, C.F., Raasch, B.A., Buettner, P.G., Weedon, D.: Accuracy of clinical diagnoses of skin lesions. British Journal of Dermatology 159, 661-668 (2008).

Iannessi, A., Beaumont, H., Hebert, C., Dittlot, C., Falewee, M.N.: Computer tomography-based body surface area evaluation for drug dosage: Quantitative radiology versus anthropomorphic evaluation. PLoS ONE 13(2): e0192124. https://doi.org/10.1371/journal.pone.0192124 (2018).

International Agency for Research on Cancer, World Health Organization: IARC Monograph on the evaluation of carcinogenic risks to human: Solar and ultraviolet Radiation. Vol. 55, Lyon (1992).

Kerby, D. The simple difference formula: an approach to teaching nonparametric correlation. Comprehensive Psychology. 3(1), 1-9 (2014).

Lague, D., Brodu, N., Leroux, J.: Accurate 3D comparison of complex topography with terrestrial laser scanner: application to the Rangitikei canyon (N-Z). J Photogramm Remote Sens. 82, 10-26 (2013).

Lavoué, G., Corsini, M.: A comparison of perceptually based metrics for objective evaluation of geometry processing. IEEE Transaction on Multimedia, 12 (7), 636-649 (2010).

Lee, J., Choi, J., Kim, H.: Determination of Body Surface Area and Formulas to Estimate Body Surface Area Using the Alginate Method. Journal of Physiological Anthropology, 27(2), 71-82 (2008).

Lee, J., Choi, J.: Estimation of Regional Body Surface Area Covered by Clothing. Journal of the Human-Environmental System, 12(1), 35-45 (2009).

Lucas, R., McMichael, A., Smith, W., Armstrong, B.K.: Solar Ultraviolet Radiation: Global burden of disease from solar ultraviolet radiation. Environmental Burden of Disease Series No. 13 (Prüss-Üstün A., Zeeb H., Mathers C., Repacholi M., eds). World Health Organization, Geneva (2006).

Mitsuhashi, N., Fujieda, K., Tamura, T., Kawamoto, S., Takagi, T., Okubo, K.: BodyParts3D: 3D structure database for anatomical concepts. Nucleic acids research, 37(Database issue), D782-5 (2008).

Pheasant, S. Bodyspace: Anthropometry, Ergonomics and design of work. Taylor & Francis, New York, 15(45), 174-93 (1996)

Raasch, B., Maclennan, R., Wronski, I., Robertson, I.: Body site specific incidence of basal and squamous cell carcinoma in an exposed population, Townsville, Australia. Mutat Res. 422(1), 101-6 (1998).

Sendroy, J., Cecchini, L. Determination of human body surface area from height and weight. Journal of Applied Physiology. 7(1), 1-12 (1954).

Standards Australia/Standards New Zealand: AS/NZS 4399:1996 Sun Protective Clothing — Evaluation and Classification. Standards Australia, Sydney and Standards New Zealand, Wellington (1996).

Standards Australia: AS/NZS 4399:2017 Sun Protective Clothing – Evaluation and Classification (2017). http://www.standards.org.au/, last accessed April 2018.

Stokes, R., Diffey, B.: How well are sunscreen users protected? Photodermatol Photoimmunol Photomed 13(5-6), 186-8 (1997).

The British Standards Institution: BS 7949:1999 Children's clothing. Requirements for protection against erythemally weighted solar ultraviolet radiation (1999). https://shop.bsigroup.com/ProductDetail/?pid=000000000030159040 , last accessed April 2018.

Tomczak, M., Tomczak, E. The need to report effect size estimates revisited. An overview of some recommended measures of effect size. Trends in sport sciences. 1(21), 19-25 (2014).

van der Pols, JC., Williams, GM., Pandeya, N., Logan, V., Green, AC.: Prolonged prevention of squamous cell carcinoma of the skin by regular sunscreen use. Cancer Epidemiol Biomarkers Prev 15(12), 2546-2548 (2006).

Venables, W.N., Smith, D.M., R Core Team: An Introduction to R. Notes on R: A Programming Environment for Data Analysis and Graphics. Version 3.4.4. R Foundation (2018). https://cran.r-project.org/manuals.html , last accessed April 2018.

Vogel, R.I., Strayer, L.G., Engelman, L., Nelson, H.H., Blaes, A.H., Anderson, K.E., Lazovich, D.: Sun Exposure and Protection Behaviors among Long-term Melanoma Survivors and Population Controls. Cancer Epidemiol Biomarkers Prev. 26(4), 607-613 (2017).

Zadeh, L.: From Computing with numbers to Computing with Words – From Manipulation of Measurements to Manipulation of Perceptions. IEEE Transactions on Circuits and Systems –Fundamental Theory and Applications, 45(1), 105-199 (1999)

Tables

Table 1. All-in-one clothing: body surface area covered (%) stratified by gender, age group and waist circumference percentile.

	Male			Female		
	Waist Circumference percentiles			Waist Circumference percentiles		
Age group (yrs)	5^{th}	50^{th}	95^{th}	5^{th}	50^{th}	95^{th}
20-29	48.30	49.08	52.06	53.73	54.90	56.96
30-39	48.76	49.75	52.06	53.70	55.02	56.94
40-49	49.05	50.56	52.87	53.31	54.85	56.66
50-59	49.27	50.82	53.12	53.00	54.54	56.47
60-69	49.53	51.26	53.66	52.74	54.38	56.27
70-79	49.85	51.52	54.44	52.44	54.09	56.10

Table 2. Comparing WBSA of DHM subjects and the results reported by Lee, Choi and Kim (2008)

		Ethnicity					
		Caucasian			*Ethic group equally represented*		
Gender	**Model**	**Nomenclature**	**Kerby's formula r_k (%) (Equation 5)**	**Median of the WBSA differences between groups MD(A)* (dm^2)**	**Nomenclature**	**Kerby's formula r_k (%) (Equation 5)**	**Median of the WBSA differences between groups MD(A)* (dm^2)**
Female	*1*	***Fm1c***	50	0.095	***Fm1m***	47	-3.259
Male	*1*	***Mm1c***	57	3.370	***Mm1m***	46	-1.533
Female	*2*	***Fm2c***	47	-3.115	***Fm2m***	47	-3.259
Male	*2*	***Mm2c***	57	3.551	***Mm2m***	51	0.102

$(*)\ MD(A) = median(A_1..A_n);\ A_i = [WBSA_{DHM\ subject\ (i)} - WBSA_{Validation\ data\ subject\ (i)}]$

Figures

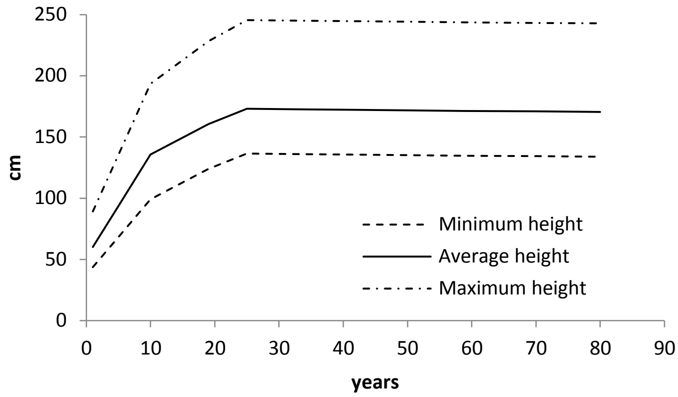

Fig. 1. Minimum, average and maximum height vs age for the male gender in MakeHuman (redrawn from Briceno, Harrison and Paul, 2018)

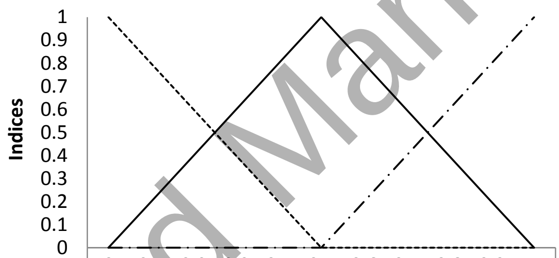

Height index	0	0.1	0.2	0.3	0.4	0.5	0.6	0.7	0.8	0.9	1
Minimum	1	0.8	0.6	0.4	0.2	0	0	0	0	0	0
Average	0	0.2	0.4	0.6	0.8	1	0.8	0.6	0.4	0.2	0
Maximum	0	0	0	0	0	0	0.2	0.4	0.6	0.8	1

Fig. 2. Membership functions for the height parameter in MakeHuman (redrawn from Briceno, Harrison and Paul, 2018)

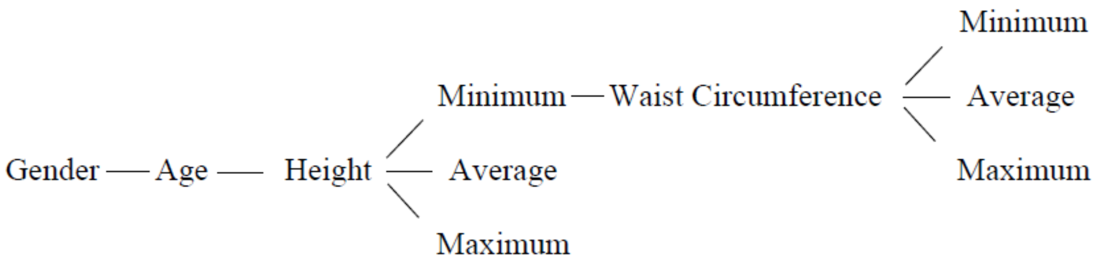

Fig. 3. MakeHuman: dependencies among parameters

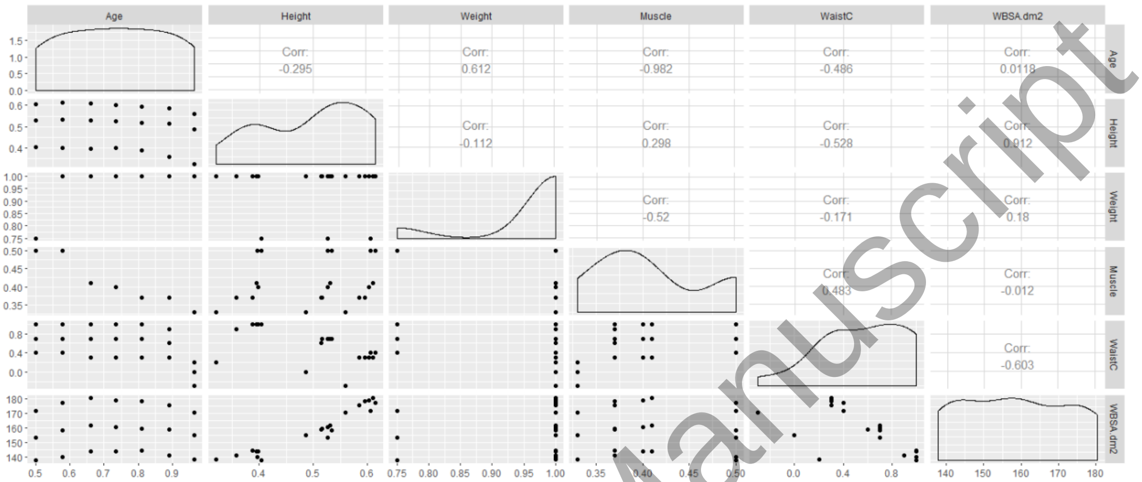

Fig. 4. Complete correlation matrix for Model 1. Female (5th, 50th and 95th) percentile height index; 50th percentile waist circumference index

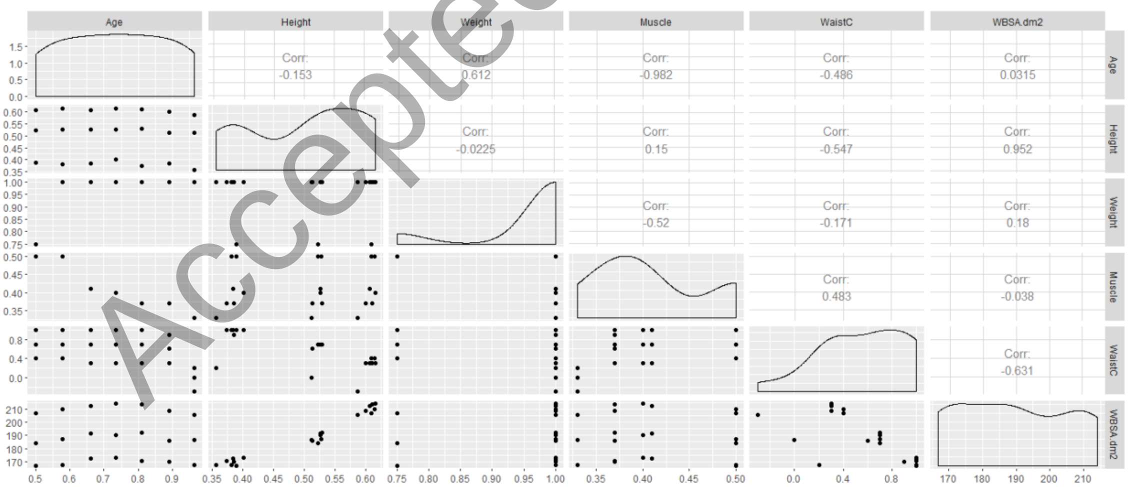

Fig. 5. Complete correlation matrix for Model 1. Male (5th, 50th and 95th) percentile height index; 50th percentile waist circumference index

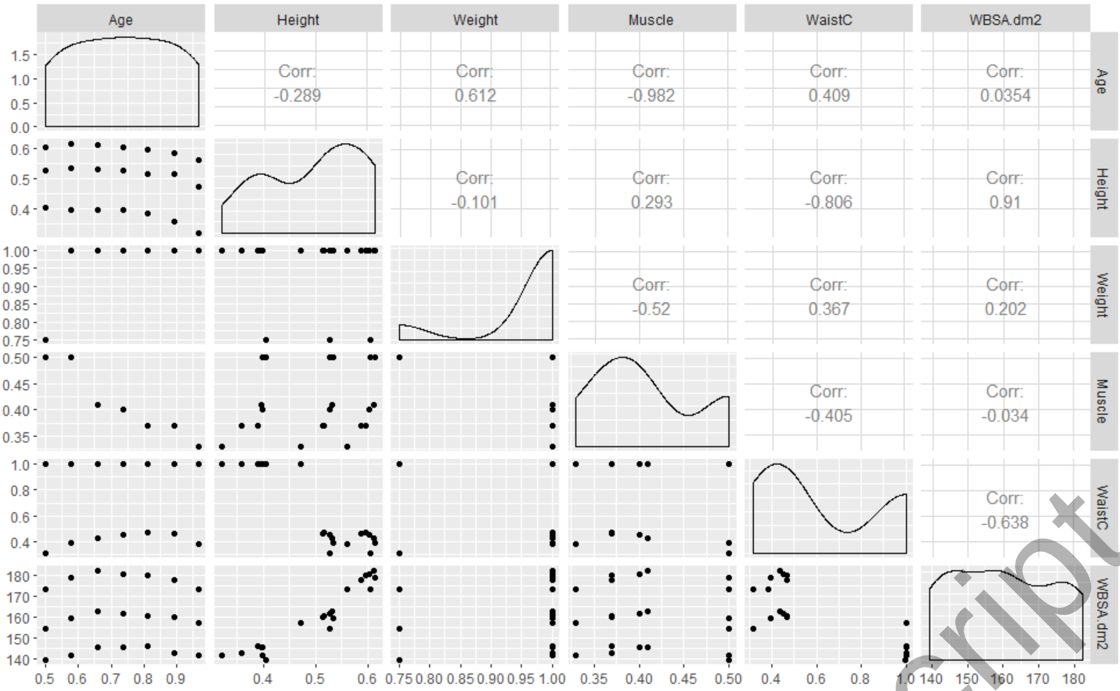

Fig. 6. Complete correlation matrix for Model 2. Female (5th, 50th and 95th) percentile height index; 50th percentile waist circumference index

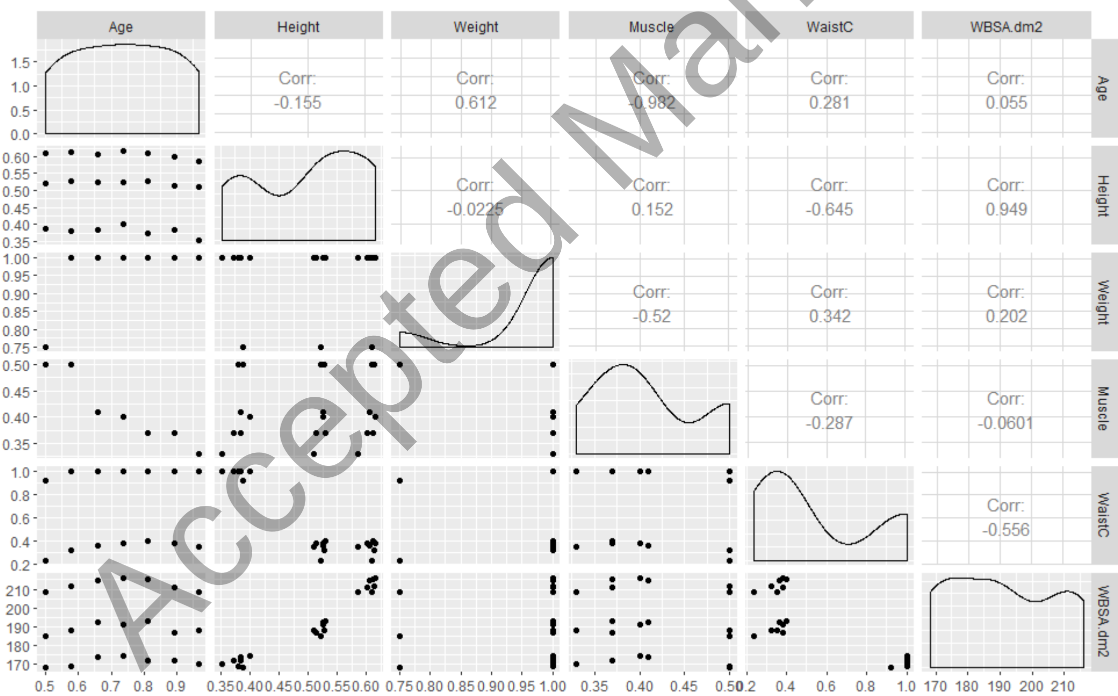

Fig. 7. Complete correlation matrix for Model 2. Male (5th, 50th and 95th) percentile height index; 50th percentile waist circumference index

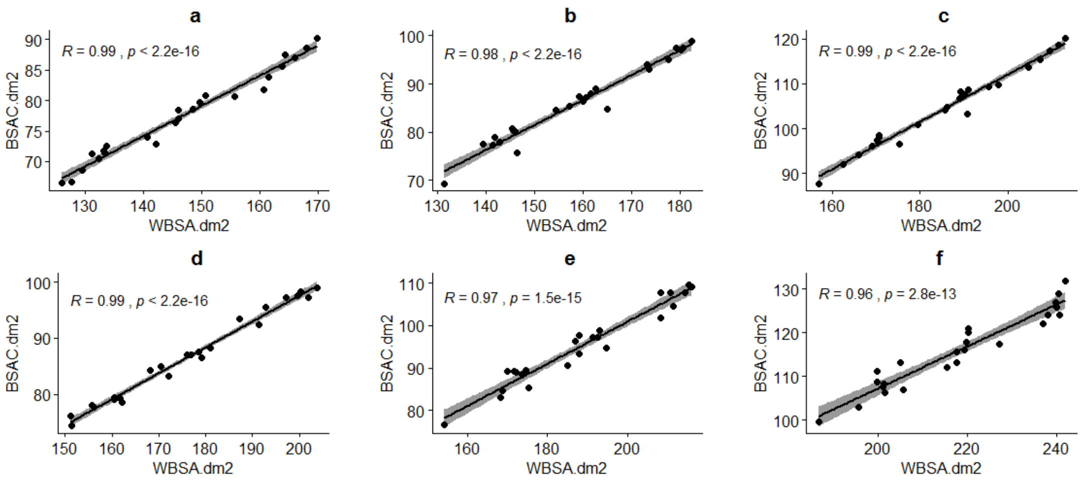

Fig. 8. Correlations between BSAC and WBSA by gender and waist circumference percentile: Females (a) 5th, (b) 50th, (c) 95th and Males (d) 5th, (e) 50th, (f) 95th

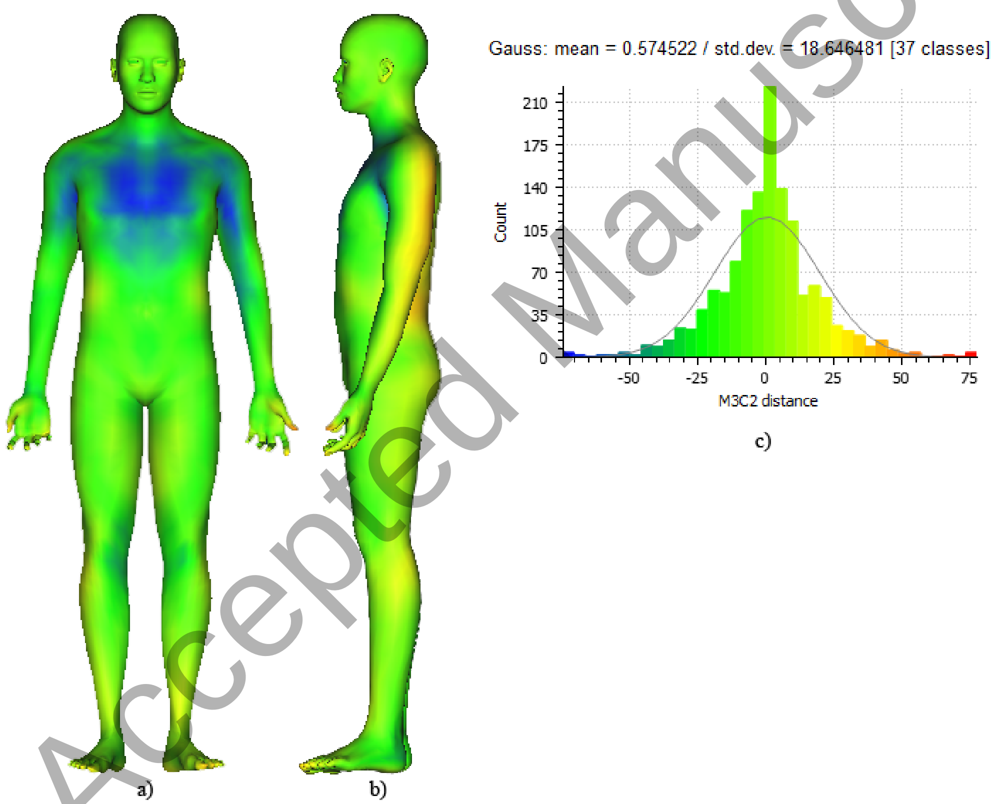

Fig. 9. M3C2 distance map, graph of the discrepancy between the scanned body (Mitsuhashi et al. 2008) and the DHM subject (a) Front view (b) lateral view (c) Histogram M3C2 distances (mm)

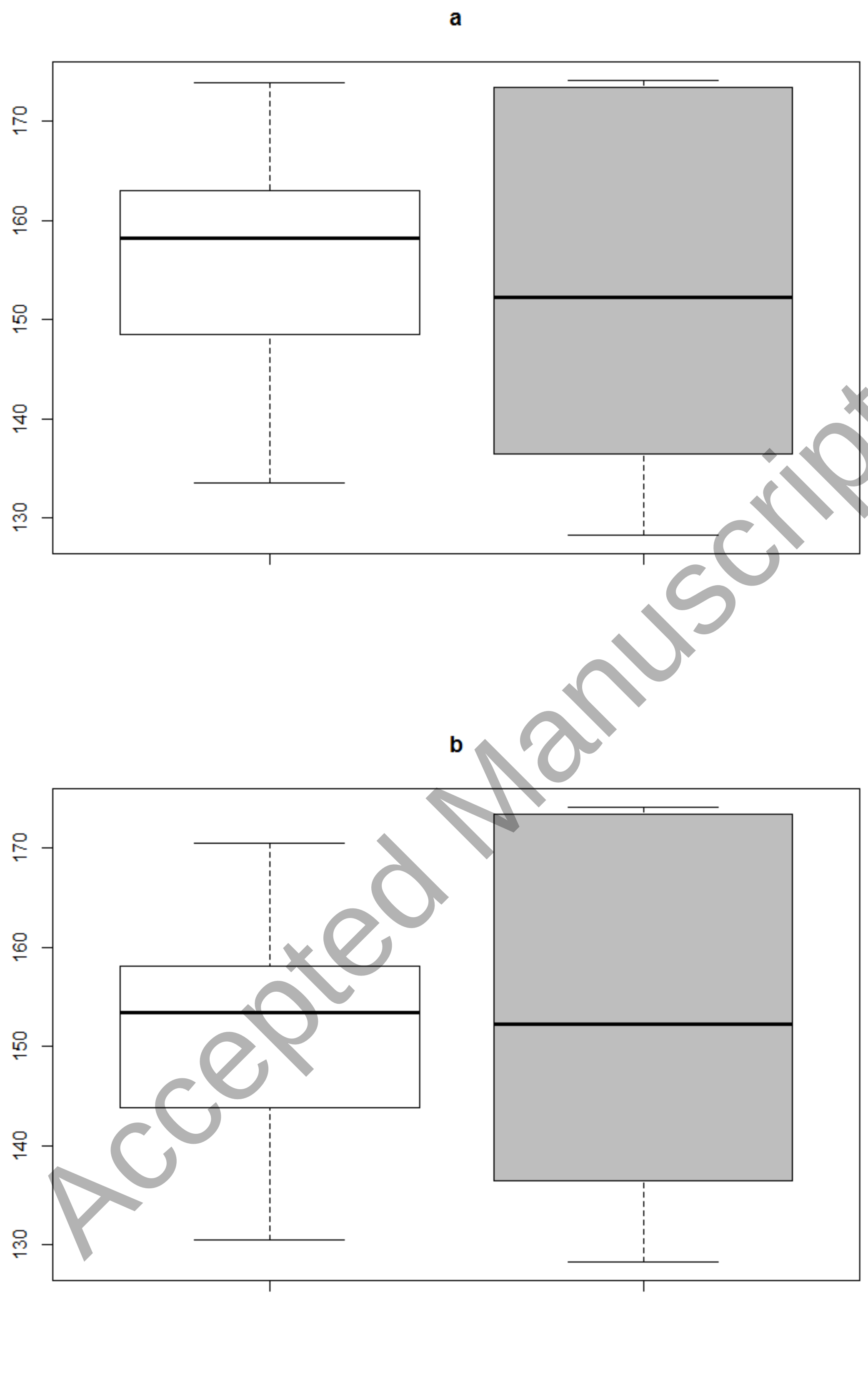
a
170
160
150
140
130
b
170
160
150
140
130

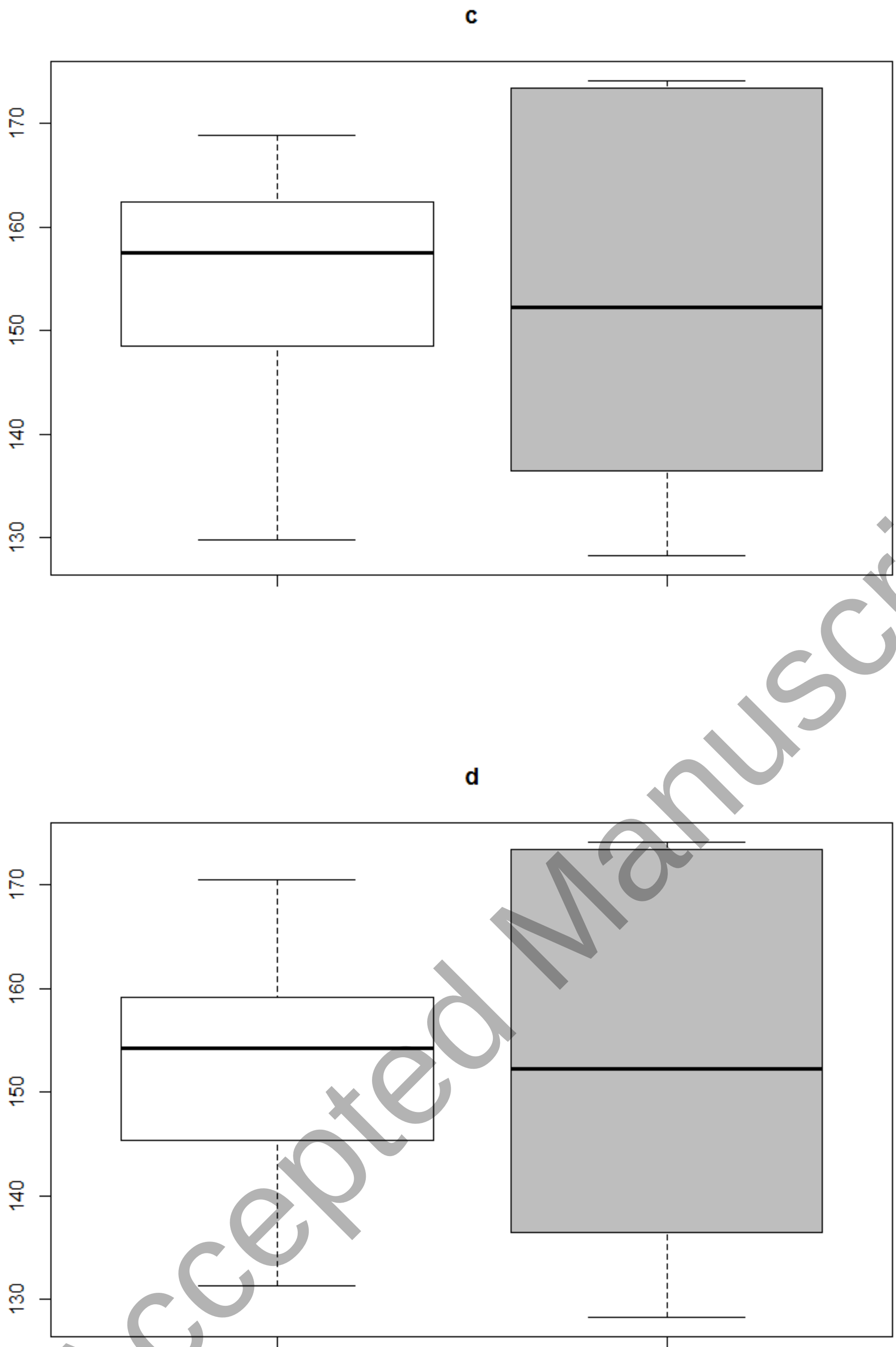

Fig. 10. Distributions of WBSA by DHM subjects and the results reported by Lee, Choi and Kim (2008), using proposed models. For female subjects: (a) Fm1c (b) Fm1m (c) Fm2c (d) Fm2m (datasets nomenclature, see Table 2). Left: DHM subject; Right: Validation study derived female data (gold standard). All values in [dm^2]

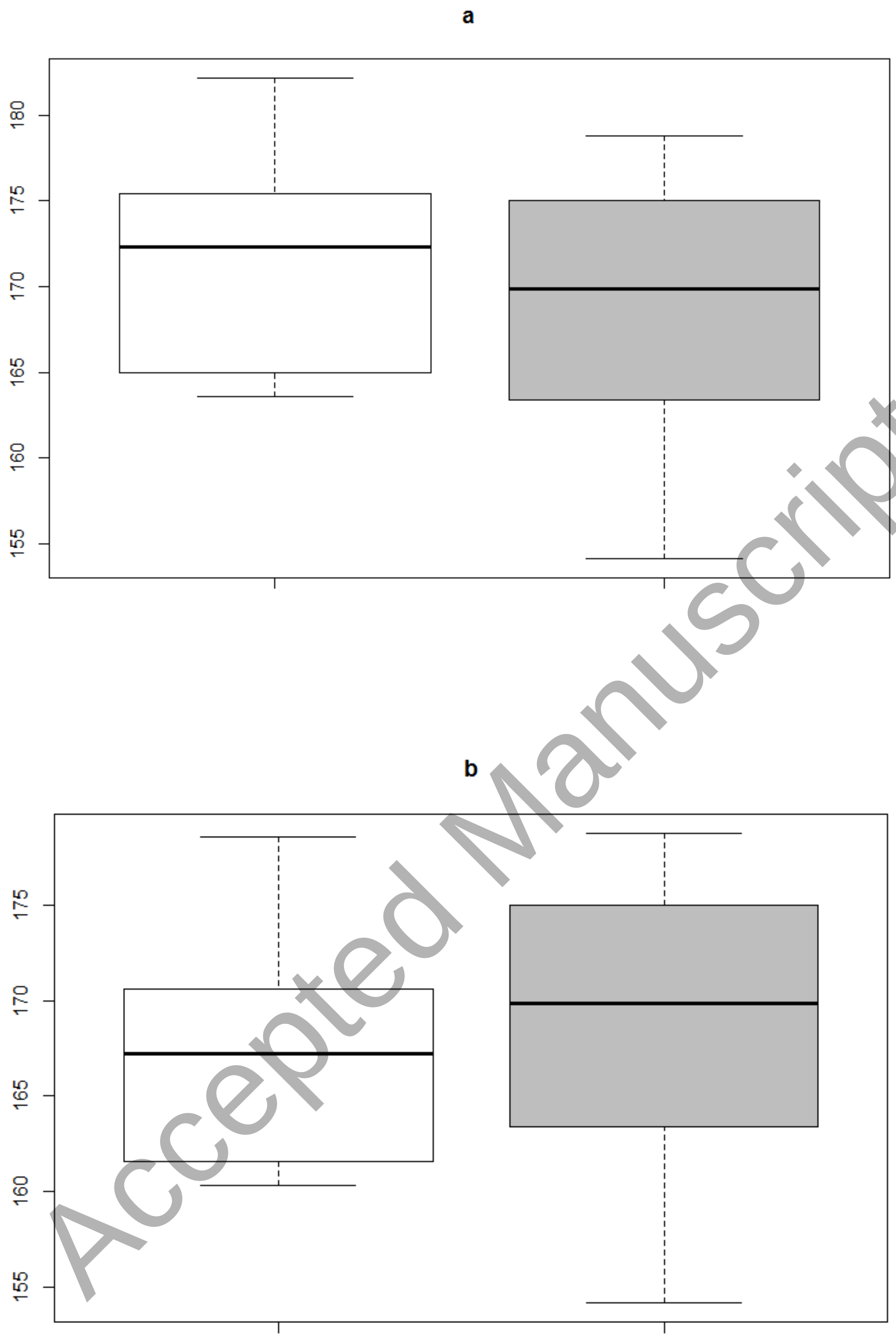
a
180
175
170
165
160
155
b
175
170
165
160
155

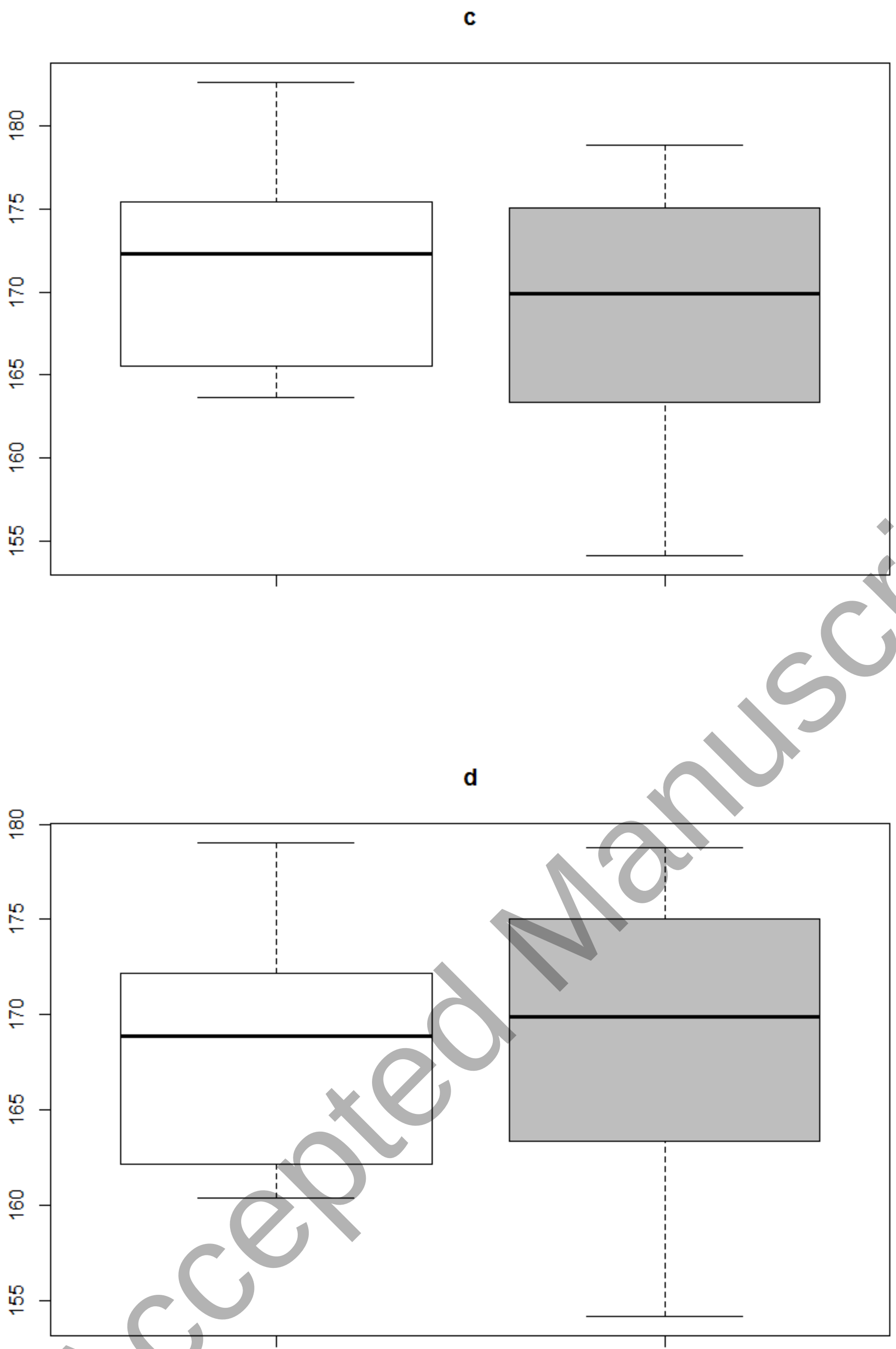

Fig. 11. Distributions of WBSA by DHM subjects and the results reported by Lee, Choi and Kim (2008), using proposed models. For male subjects: (a) Mm1c (b) Mm1m (c) Mm2c (d) Mm2m (datasets nomenclature, see Table 2). Left: DHM subject; Right: Validation study derived male data (gold standard). All values in [dm^2]